Structure and Stability of Fe Nanocrystals: An Atomistic Study

ARTICLE *in* THE JOURNAL OF PHYSICAL CHEMISTRY C · OCTOBER 2010

Impact Factor: 4.77 · DOI: 10.1021/jp107709q

Structure and Stability of Fe Nanocrystals: An Atomistic Study

Yang Zhang,[†] Yu-Hua Wen,*[,†] Zi-Zhong Zhu,[†] and Shi-Gang Sun*[,‡]

Department of Physics and Institute of Theoretical Physics and Astrophysics, Xiamen University, Xiamen 361005, China, and State Key Laboratory of Physical Chemistry of Solid Surfaces, Department of Chemistry, College of Chemistry and Chemical Engineering, Xiamen University, Xiamen 361005, China

Received: August 15, 2010; Revised Manuscript Received: September 27, 2010

By means of atomistic simulations, we have investigated the energetics and stability of Fe nanocrystals with different crystal structures and shapes. It has been found that structural stability of Fe nanocrystals depends strongly on the size of nanocrystals. Furthermore, twinned fcc nanocrystals are energetically more stable than bcc single nanocrystals at very small sizes. Investigation on dynamics evolution of fcc Fe nanocrystals under heating reveals that the solid−solid phase transition from fcc to bcc occurs prior to the melting. The temperature of phase transformation depends on the shape of Fe nanocrystals. The bcc phase preferentially nucleates in apes of fcc Fe nanocrystals and spreads through entire ones with increased temperature. Twin structures suppress the propagation of the nucleated bcc phase, thereby, enhancing the thermal stability of twinned fcc Fe nanocrystals.

1. Introduction

As the fourth most abundant element on earth, iron (Fe) is the most widely used of all the metals.[1] Its high strength, high reactivity, low cost, and ferromagnetism make it indispensable in industrial applications such as the construction of machinery, catalysts, and magnetic recording media.[2−4] Fe has three distinct polymorphs: the body-centered cubic (bcc), the face-centered cubic (fcc), and the hexagonal close packed (hcp). Extensive studies demonstrate that Fe exhibits the ferromagnetic bcc phase (α-Fe) under ambient conditions, and transforms into paramagneticβ-Fe with the same structure above 1043 K.[5] The fcc structure (γ-Fe) is stable at temperatures above 1185 K, whereas the bcc structure (δ-Fe) reoccurs above 1667 K and melts into liquid state at 1811 K.[5] The bcc α-Fe can experience a fully reversible phase transition to the hcp structure (ε-Fe) at room temperature and pressure of 13 GPa.[6] The phase transition between bcc and hcp structures is particularly important for geophysicists to explore the phase composition and seismic structure of the iron-rich core of the Earth.[7,8] The phase transition between fcc and bcc structures, however, plays a key role in metallurgy and crystallography for controlling the microstructure, morphology, and fabrication of iron and iron alloys.[9−11]

Fcc bulk Fe is important but thermodynamically unstable at ambient conditions. Many attempts have been made in the past to stabilize the fcc structure of Fe specimens at room temperature. An effective approach is to decrease the size of Fe materials, which has been confirmed by the fact that Fe single crystals with nanoscale size and fcc structure, grown within graphitic nanotubes, remained structurally stable and exhibited ferromagnetic at room temperature.[3] Fcc Fe nanocrystals with novel twinned structures have also been synthesized successfully.[12,13] These results have confirmed that the stability of Fe materials is not only associated with their crystalline structures but also their sizes. With decreasing sizes to the nanoscale level, Fe particles are formed by a reduced number of atoms and the majority of them are located at the surface. The atomic arrangement and coordination of surface, determined by crystal shape and surface Miller index, will play a key role in determining their fundamental, physical, and chemical properties. It is known that the surface energy of different crystalline planes for fcc metals is increased in the order of $\gamma_{\{111\}} < \gamma_{\{100\}} < \gamma_{\{110\}}$, whereas for bcc metals is $\gamma_{\{110\}} < \gamma_{\{100\}} < \gamma_{\{111\}}$.[14,15] Therefore, it is expected that Fe nanocrystals enclosed by planes of low energy will possess a lower total surface energy and better stability compared with other Fe nanocrystals, as evidenced by experimental results.[4,12,13,16] Recently, cubic and dodecahedral bcc Fe nanocrystals enclosed with six {100} and twelve {110} facets were successfully prepared by means of an electrochemical route;[4,16] cubic and tetrahedral fcc Fe nanocrystals covered by six {100} and four {111} facets were also synthesized through mild reduction combined with heating method.[12,13] It has demonstrated that the icosahedral and decahedral Fe nanocrystals with twinned fcc structures exhibit good stability when their sizes go down below tens of nanometers.[12,13] Such stability has been attributed to their enclosed {111} facets that minimize the total surface energy. These studies have prompted the development of Fe nanocrystals and attracted wide interests of research.

Despite the fact that Fe nanocrystals have been extensively investigated over the past decade,[2−4,11−13,16−18] to the best of our knowledge, a thorough study of stability analysis by a consideration of Fe nanocrystals with different sizes and shapes is currently lacking. Moreover, a strong doubt arises spontaneously after successful synthesis of unusual fcc Fe nanocrystals, that is what will happen to these Fe nanocrystals stable at room temperature when they are subjected to heating or put in high temperature conditions? Whether they can retain their original shape and structures is a vital factor for their final applications. Especially, there is a rather complicated dynamics process under heating for bulk Fe because this process is associated with multiphase transformation and competition. Although the real-time in situ visualization of phase transformation from bcc to fcc structures in Fe thin-film has been reported recently,[11] it is

* To whom correspondence should be addressed. E-mail: yhwen@xmu.edu.cn (Y.-H.W.), sgsun@xmu.edu.cn (S.-G.S.).

[†] Department of Physics and Institute of Theoretical Physics and Astrophysics.

[‡] Department of Chemistry.

10.1021/jp107709q
Published on Web 10/19/2010

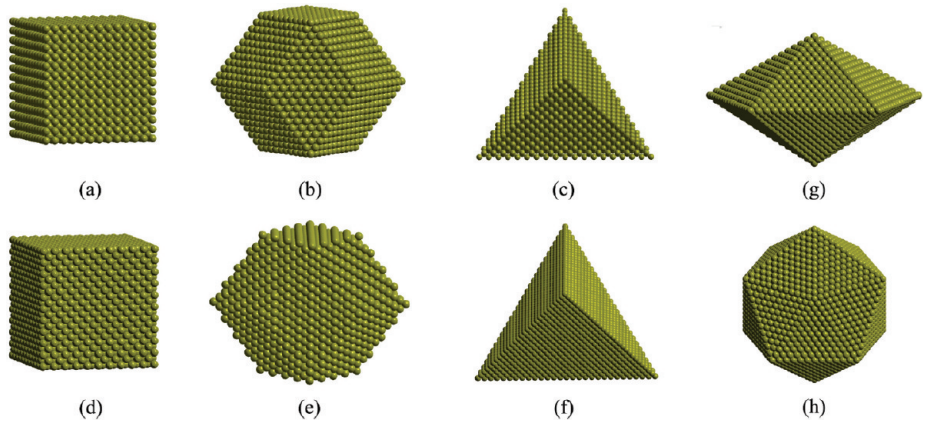

Figure 1. Schematic illustration of bcc Fe nanocrystals (a) cube, (b) dodecahedron, (c) tetrahedron; fcc Fe nanocrystals (d) cube, (e) dodecahedron, (f) tetrahedron; and twined fcc nanocrystals (g) decahedron, (h) icosahedron.

still a fundamental challenge to directly monitor and capture the dynamics process of phase transition in Fe nanocrystals because of their tiny 3D scales making the manipulation rather difficult.

In this article, we have focused on studies of structure and stability of Fe nanocrystals by means of atomistic simulations. Strong size dependence of structural stability is revealed in these nanocrystals. We find that the martensitic transformation from fcc to bcc phase is possible for defect-free fcc Fe nanocrystals under heating process. Furthermore, twin structures may enhance their thermal stability through suppressing the development of bcc nucleus. These results highlight the importance of controlling the synthesis temperature and crystal shape so that Fe nanocrystals with better thermal stability could be obtained.

2. Simulation Methodology

As mentioned above, those Fe nanocrystals enclosed by planes of low energy such as {110} and {100} for bcc, {100} and {111} for fcc crystals, will demonstrate better stability compared with other Fe nanocrystals.[4,12,13,16] Therefore, here have been considered six types of Fe nanocrystals, namely cubic, tetrahedral, and decahedral ones with bcc and fcc single crystals, respectively. Because of the twin structures lowering the total surface energy of Fe nanocrystals at small size,[12,13] decahedral and icosahedral fcc Fe nanocrystals with 5-fold twinned structures, enclosed by {111} facets, have also been considered in this study. These eight types of Fe nanocrystals have been illustrated schematically in Figure 1. Similarly, a series of Fe nanocrystals with different sizes are modeled in this article. Because of the limitation of present computer facilities available, the total number of atoms in Fe nanocrystals varies between 200 and 220 000 atoms.

In atomistic computer simulations, the atomic interactions of iron are described by the Finnis−Sinclair many-body potentials,[19] which are based on the second-moment approximation of the tight-bonding formulation. These potentials represent many-body interactions, and their parameters are optimized to describe the lattice parameter, cohesive energy, bulk modulus, elastic constants, vacancy formation energy, stacking-fault energy, and pressure-volume dependency. They have been confirmed to reproduce very well the basic structural and dynamics properties of iron.[20,21]

Upon starting the dynamics simulations, all the Fe nanocrystals have been first relaxed to a local minimum energy state by using the conjugate gradient method (CGM).[21] The cohesive energy of each nanocrystal can be obtained by summing the total energy of atoms in the nanocrystal. After full relaxation, these nanocrystals are subjected to a heat processing. To make the simulations more realistic, we employ constant temperature molecular dynamics (NVT-MD) to allow energy fluctuations, which may be critical to the resulting dynamics. These nanocrystals undergo the heating process from 0 to 2100 K with temperature increment of 20 K. The simulations are carried out for 200 ps of the relaxation time at each temperature. The desired temperature is maintained by Nose−Hoover thermostat,[22] and the equations of atomic motion are integrated by the Verlet-Velocity algorithm[23] with a time step of 1.0 fs.

3. Results and Discussion

For comparison of Fe nanocrystals with different shapes and structures, a common definition of crystal size, based on equivalent volume, has been introduced as follows:

$$d = \sqrt[3]{0.5N}a_0 \tag{1}$$

where N and $a_0 = 2.8665$ Å are total number of Fe nanocrystals and lattice constant of bcc bulk Fe. Figure 2 shows the size dependence of the cohesive energy for the fully relaxed nanocrystals of size up to 14 nm. As seen in the figure, strong size effects are evident for all types of Fe nanocrystals. By comparison of cohesive energy, bcc Fe nanocrystals of dodecahedral form are found to be most stable but bcc Fe nanocrystals of tetrahedral form are most unstable in all of the nanocrystals considered. This result is not surprising because the surface energy of {110} of bcc crystal is the lowest among all planes of Fe single crystal.[15] In the case of cubic and dodecahedral single nanocrystals, the bcc structure is more stable than the fcc structure. However, the tetrahedral Fe nanocrystals show more energetically stable for fcc structure than bcc structure when the crystal size is below 11 nm. This indicates that surface effects will play a dominant role in determining the stability of Fe nanocrystals compared with crystal structure under ultrafine crystal sizes. Surprisingly, the twinned fcc Fe icosahedral and decahedral nanocrystals exhibit better stability than fcc single crystalline cubic and tetrahedral ones when the crystal sizes are below tens of nanometers.

It is learned from the above description that the cohesive energy of Fe nanocrystals depends on both their surface structures and their sizes. To further investigate the size effects on structure and stability of Fe nanocrystals, we express the cohesive energy by consideration of nanocrystal composition.

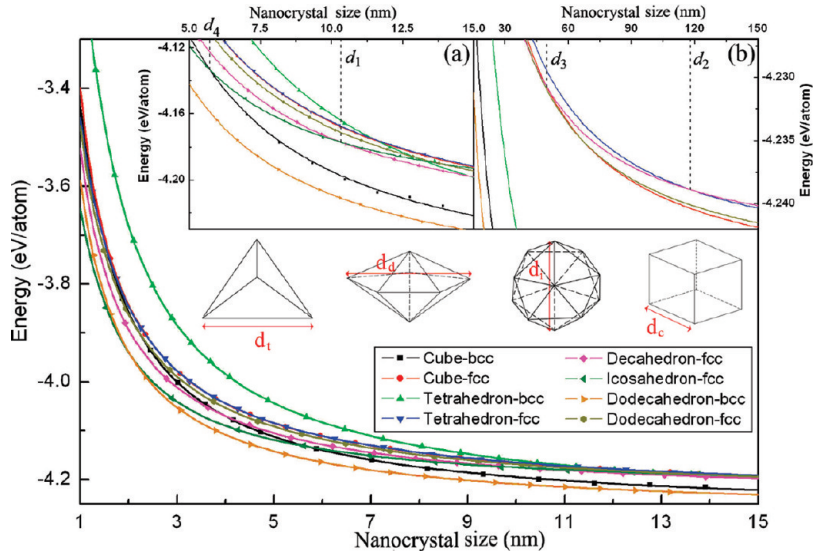

Figure 2. Energy as a function of nanocrystal size at small size from 1 to 14 nm. Inserted pictures: (a) the energy vs crystal size enlarged from Figure 2, (b) the results of Fe nanocrystals with large size between 15 and 150 nm predicted from the fit curves.

Considered that a polyhedral nanocrystal can be composed of atoms located in its interior, facets, edges, and vertices, the average energy per atom of nanocrystal can be expressed as

$$\bar{E} = \frac{1}{N}(N_i\bar{E}_i + N_f\bar{E}_f + N_e\bar{E}_e + N_v\bar{E}_v) = A + \frac{B}{d} + \frac{C}{d^2} + \frac{D}{d^3} \quad (2)$$

where N, N_i, N_f, N_e, and N_v are the atomic number of the system, interior, facets, edges, and vertices, respectively; $\bar{E}$, $\bar{E}_i$, $\bar{E}_f$, $\bar{E}_e$, $\bar{E}_v$ is the average energy per atom of the system, interior, facets, edges, and vertices, respectively. Herein, we adopt the quartic-type functions above to fit the data of calculations with the framework of the least-squares method, and depict the fitted curves in Figure 2. Clearly, there are three critical crystal sizes (denoted as d_1, d_2, d_3) to distinguish the stability of fcc Fe nanocrystals with different shapes. For those fcc Fe nanocrystals enclosed by {111} facets, the icosahedron is the most stable shape when the crystal size is below $d_1 = 10.3$ nm, whereas the decahedron is the most stable shape when the crystal size is between $d_1 = 10.3$ nm and $d_2 = 118$ nm, and the tetrahedron is most stable shape for the crystal size over 118 nm. Experimentally, the crystal size d is generally defined as the schematic diagram inserted in Figure 2. According to the volume of nanocrystals, we can deduce that the icosahedral nanocrystal is the most stable morphology when its size d_i is below 10.6 nm. The decahedral nanocrystal will be preferentially stable as the crystal size d_d falls into between 13.8 and 158.9 nm. When the crystal size d_t is above 165 nm, the tetrahedral nanocrystal with single crystal structure is more stable than those twinned nanocrystals. Figure 2 also illustrates that $d_3 = 49.89$ nm is the critical size between cubic and decahedral fcc Fe nanocrystals, indicating that the cubic nanocrystal will be energetically more stable than the decahedral one when its size d_c is larger than 49.3 nm. The aforementioned results show that the most stable morphology is icosahedral crystal of small crystal sizes, followed by decahedral one at mediate sizes, and cubic and tetrahedral ones at larger sizes. Our calculated results are in good agreement with experimental observations and the predication of the Gibbs free energy based on the thermodynamic method.[12,13]

It is interesting that the twinned fcc Fe nanocrystals are more stable than single fcc Fe nanocrystals at crystal size below tens of nanometers, which may be elucidated by their constructions. The fcc Fe tetrahedral crystal is the component unit of the twinned fcc Fe decahedral and icosahedral crystals. The decahedron and icosahedron are composed of five and twenty tetrahedra, respectively.[12,13] At tens of nanometers or smaller, these tetrahedral single crystals can be assembled to form the twinned fcc Fe decahedral and icosahedral crystals with larger sizes but lower energy, resulting in that the Fe nanocrystals prefer to be the form of twinned fcc Fe nanocrystals. When the crystal size is large enough so that the assembling behavior of these tetrahedral crystals does not lower their total energy, they prefer to exist individually. Therefore, the Fe crystals prefer to be the tetrahedral or other single crystal forms at large sizes. In addition to those polyhedral Fe nanocrystals, which belong to fcc structure, we have also investigated bcc Fe nanocrystals and compared their structural stability. Interestingly, there is a crossover of the cohesive energies for fcc twinned icosahedral nanocrystals and bcc single crystalline cubic ones, as shown in Figure 2. It is found that a critical size occurs at $d_4 = 5.7$ nm, suggesting that at very small sizes, fcc twinned nanocrystals are energetically more stable than bcc single nanocrystals. A confirmable fact is that bcc Fe nanocrystals with such small size are not found experimentally up to date.[4,16] It indicates that at such small size, surface effects will be pronounced and play more important roles than the crystal structure in determining the structural stability of nanocrystals.

Because of the existence of aforementioned unusual fcc Fe nanocrystals at ambient conditions, there has arisen a nature motivation to explore their thermal stability under heating or high temperature conditions. Herein, we pay our attention on the temperature dependent stability analysis of those experimentally prepared Fe nanocrystals with fcc structures, that is, cubic, tetrahedral, decahedral, and icosahedral ones. Figure 3 illustrates the temperature dependence of the potential energy as well as the specific heat capacity for the four types of nanocrystals. Generally, the temperature of solid to liquid phase transition can be identified by investigating the variation in the potential energy and specific heat capacity.[24] The overall melting points of Fe nanocrystals obtained from Figure 3 are almost equal and somewhat independent of their shapes. A similar result

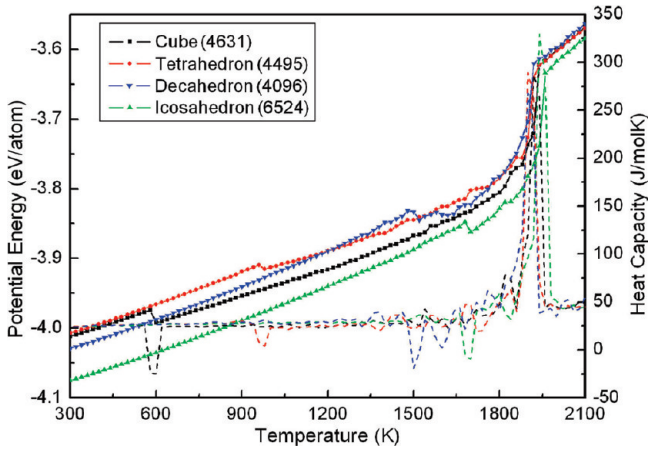

Figure 3. Potential energy and specific heat capacity of fcc Fe nanocrystals as a function of temperature. The number in parentheses denotes the total number of atoms of nanocrystal.

has occurred in Pt nanocrystals.[25] Further analyses on the melting mechanism of Fe nanocrystals show that the premelting is originated from the surface and results in the overall melting of nanocrystals at the melting point, which is consistent with Ni, Au, Ag, and Pt nanocrystals.[24−28] However, a significant difference exists between Fe and other metallic nanocrystals under heating. Different from other metallic nanocrystals whose potential energies monotonically increase with rising temperature, the potential energy of fcc Fe nanocrystals suddenly decreases when the temperature rises to a critical point before melting, which has also been identified by the negative specific heat capacity in Figure 3. The critical temperature is 580, 980, 1520, and 1680 K for the cubic, tetrahedral, decahedral, and icosahedral Fe nanocrystals respectively, demonstrating that it is strongly dependent on the crystal shape. Moreover, twinned fcc Fe nanocrystals exhibit higher critical temperatures compared with single crystalline nanocrystals.

Why do the potential energies of fcc Fe nanocrystals exhibit an sudden reduce during the heating? This should be closely associated with structural changes of these nanocrystals. To further monitor the structural evolution of Fe nanocrystals, we apply the common neighbor analysis (CNA) proposed by Honeycutt and Andersen[29] to characterize the local crystal structure. The CNA method has already been used successfully to analyze the structural evolution during the deformation process.[30,31] This analysis assigns four indices *ijkl* to each pair of atoms that have common neighbors and provides a description of the local environment of the pair. In this analysis, the bonds between an atom and its nearest neighbors are examined to determine the crystal structure. The different types of pairs are associated with different types of local order. All bonded pairs in the fcc crystal are of type 1421, whereas the hcp crystal has equal numbers of type 1421 and 1422. Both type 1441 and 1661 are the main bonded pairs in the bcc crystal. Therefore, each atom in nanocrystals can be classified according to its local crystalline structure. Considering that iron has three different crystal structures, namely bcc, fcc, and hcp, here we have classified atoms into four categories by the CNA method. Atoms in a local fcc order are considered to be fcc atoms; atoms in a local bcc order are considered to be bcc atoms; atoms in a local hcp order are classified as hcp atoms whose occurrence in fcc crystal is regarded as the structure of stacking faults; atoms in all other local orders are considered to be other atoms.

Figure 4 shows snapshots of cubic and tetrahedral Fe nanocrystals at three different temperatures under the heating process, implying the phase transformation from fcc to bcc structure. By further investigation of structural evolution, it is found that the cubic nanocrystal can retain its original fcc structure and shape up to 540 K. With the temperature increasing to 560 K, it is clearly seen from part b of Figure 4 that local bcc structures have nucleated near apexes of the cubic nanocrystal. This martensitic nucleation is heterogeneous and develops further with rising temperature. Once the nucleus has reached a critical size that is big enough to lower the energy of the barriers for additional nucleation, then the propagation of the bcc phase can rapidly follow to accomplish the martensitic transformation of entire nanocrystal, resulting in the final formation of bcc Fe nanocrystal at 580 K (part c of Figure 4). Moreover, it is found that the shape of the cubic nanocrystal changes into an approximate cuboid. The shape change can be interpreted qualitatively by the Bain path which consists of a homogeneous contraction of the cube along its two sides in three sides perpendicular to each other, and a simultaneous dilation in other side.[32] However, a high energy barrier lies in the direct transformation from fcc to bcc phase by the Bain path. In fact,

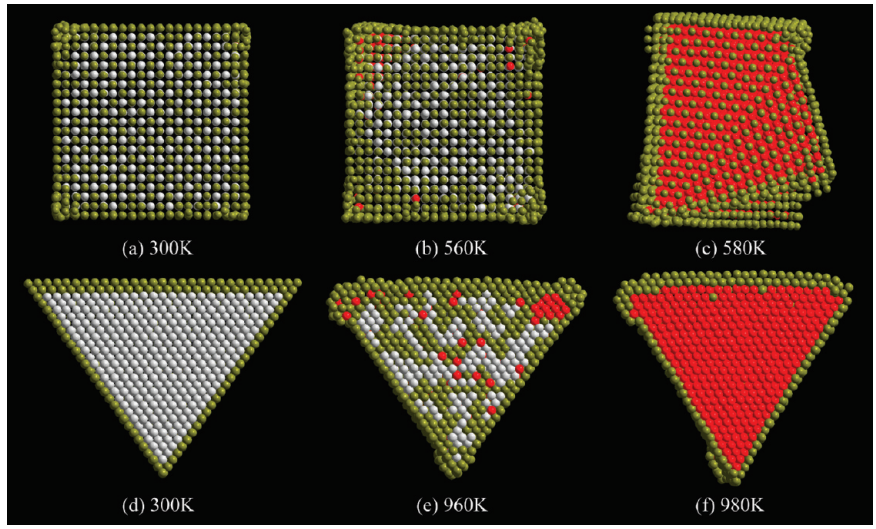

Figure 4. Snapshots of cubic (up) and tetrahedral (down) fcc Fe nanocrystals at three representative temperatures in heating process. Note that a small atomic radius in cubic nanocrystal and cross sections in tetrahedral nanocrystal are applied to highlight the phase transition. Coloring denotes local structure: light gray, fcc; red, bcc; blue, hcp; and dark yellow, other.

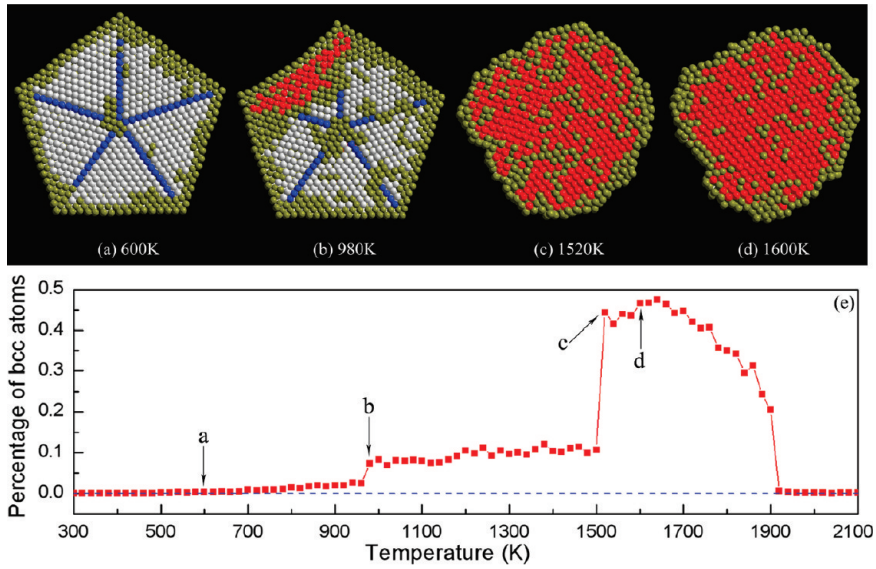

Figure 5. (a)−(d) Snapshots of cross sections of fcc Fe decahedral nanocrystal at four temperatures in heating process. (e) Temperature dependence of the percentage of bcc atoms for fcc Fe decahedral nanocrystal. Coloring denotes local structure: light gray, fcc; red, bcc; blue, hcp; and dark yellow, other.

the martensitic transformation is realized by the multislip events, involved in a series of jumps and rearrangements by a group of atomic displacements in the cubic nanocrystal, which has been verified by the irregular cuboid of Fe nanocrystal in part c of Figure 4 after full transformation. A similar mechanism of phase transition can be found in tetrahedral nanocrystal (parts d−f of Figure 4). The difference is that the tetrahedral nanocrystal exhibits higher temperature of the martensitic transformation than the cubic one. This should be attributed to those atoms with high coordination number and stable configuration in the fcc tetrahedral nanocrystal enclosed by {111} surfaces, making the nucleation of bcc structure difficult. Therefore, higher temperature is necessary to overcome the energy barrier for the nucleation of bcc structure in the tetrahedron.

It is worth noting that higher transition temperatures have occurred in twinned fcc Fe nanocrystals compared with the tetrahedral one (Figure 3). It is 540 and 700 K higher for decahedral and icosahedral nanocrystals than for the tetrahedral one respectively, although all of them are enclosed by the same {111} facets. High transition temperatures indicate that the decahedral and icosahedral nanocrystals have a better thermal stability in comparison with the tetrahedral one. To further explore the mechanism of their phase transition, the twinned fcc decahedral nanocrystal is first subjected to a heating process. Four representative atomic configurations of the decahedral nanocrystal at different temperatures are illustrated in Figure 5. At low temperature, the decahedral nanocrystal can retain its original shape and structure (part a of Figure 5). However, the bcc phase first nucleates, and then enlarges in one of the five fcc tetrahedra included in the twinned decahedron at 980 K, as illustrated by part b of Figure 5. The propagation of the bcc phase is then hindered with further heating when it meets twin boundaries of nanocrystal, which has been confirmed by the fact that the percentages of bcc atoms do not increase significantly up to 1500 K (part e of Figure 5). The nanocrystal has transformed completely to bcc phase and the initial twin boundaries have disappeared simultaneously at 1520 K. At the moment, some lattice misfits can be found in bcc Fe nanocrystal, as shown in part c of Figure 5. They have disappeared by atomic rearrangements with further heating. Part d of Figure 5 depicts the final formation of a complete bcc nanocrystal at 1600 K. We find that this mechanism of phase transition keeps valid in the icosahedral nanocrystal. It is also observed that the bcc structure originates and nucleates preferentially in one of the twenty fcc tetrahedra included in the twinned icosahedron at 980 K. Because of the fact that larger percentage of twins in the icosahedron makes the propagation of the bcc phase through twin boundaries more difficult, the twinned icosahedral nanocrystal exhibits therefore the highest transition temperatures in all the nanocrystals enveloped by {111} facets.

The aforementioned results indicate that the presence of twin boundaries can obstruct the propagation of the nucleated bcc phase, suppressing the development of martensitic transformation. As illustrated in part a of Figure 5, the crystalline orientations of adjacent fcc tetrahedra beside twin boundary are different. After the bcc phase is nucleated in one of the five fcc tetrahedra, its development will be suppressed when it meets the twin boundary. For further propagation, it must overcome the obstruction of twin boundary and crystal mismatch in adjacent tetrahedra, resulting in the suppression of solid−solid martensitic transformation. Therefore, on the one hand twin boundaries can enhance the thermal stability of twinned Fe nanocrystals to a certain extent. Their presence may be nevertheless disadvantageous for the stability, on the other hand. Those atoms located in twin boundaries usually have higher energy and lower coordination number compared with the bulk atoms. With the temperature increasing to a sufficiently high value, they will be easily diffusive and preferentially become disorder, leading to the premelting near twin boundaries.[33] The boundary energy can be increased due to premelting, associated with a localized disorder of the atoms near the grain boundary energy.[34] It is known that the solid−liquid phase transition is controlled by the diffusive behavior, hence the presence of twin boundary weakens the thermal stability of nanocrystals. However, our calculations indicate that the solid−solid martensitic transformations are mainly driven by displacements, which rely on more ordered cooperative movements of many atoms to induce changes in the crystal shape and/or structure.[35] Furthermore, the twin boundaries have already been disappeared before the occurrence of melting. In this case, the presence of twin structures may strengthen the thermal stability of nanocrystals.

It should be noted that in the bulk, it is not easy to trigger solid−solid phase transitions by heating or cooling via molecular dynamics simulations.[36] The inclusion of high defect densities is necessary for these phase transitions. The solid−solid transformations do not also happen in the large nanocrystals without defects.[37] However, at small sizes, large surface-to-volume ratio and high surface free energy could play a key role in the determination of the phase transition of the nanocrystals. Our results have revealed that high percentage of surface atoms may be beneficial to the nucleation of new phase and the process of solid−solid phase transitions although the interior of nanocrystal has no defects and vacancies.

4. Conclusions

In this article, the stability of polyhedral Fe nanocrystals with different shapes and structures has been investigated by atomistic simulations. The results have revealed that the structural stability of Fe nanocrystals is strongly dependent on their sizes and shapes. A comparison of the results with those experimental observations and thermodynamic calculations presents a good consistency. Furthermore, at very small sizes (below 5.7 nm), twinned fcc icosahedral nanocrystals are energetically more stable than bcc single nanocrystals. Further investigation on dynamics process of fcc Fe nanocrystals under heating conditions has demonstrated that the solid−solid phase transition from fcc to bcc occurs prior to the melting. The bcc phase prefers to nucleate in the apes of nanocrystals and propagate through entire nanocrystals with increased temperature, which results in the final completion of phase transition. The presence of twin boundaries can hinder the propagation of the nucleated bcc phase, enhancing the thermal stability of twinned fcc decahedral and icosahedral Fe nanocrystals. Our simulations have demonstrated that high percentage of surface atoms may be responsible for the phase transition of fcc Fe nanocrystals with ultrafine sizes. These results are expected to motivate future experimental attempts by controlling the synthesis temperature and crystal shape to prepare Fe nanocrystals with better thermal stability and to tailor their catalytic properties at the nanoscale.

Acknowledgment. This work is supported by NSFC (Grant Nos. 20833005, and 10702056), the MOST (Grant No. 2007DFA40890) and Fujian Provincial Department of Science and Technology (Grant No. 2008I0025). Y. Z. thanks the Ph.D. program of Xiamen University for support.

References and Notes

(1) Andrault, D.; Fiquet, G.; Kunz, M.; Visocekas, F.; Hausermann, D. *Science* **1997**, *278*, 831–834.

(2) Huber, D. L. *Small* **2005**, *1*, 482–501.

(3) Wei, B. Q.; Shima, M.; Pati, R.; Nayak, S. K.; Singh, D. J.; Ma, R. Z.; Li, Y. B.; Bando, Y.; Nasu, S.; Ajayan, P. M. *Small* **2006**, *2*, 804–809.

(4) Chen, Y. X.; Chen, S. P.; Zhou, Z. Y.; Tian, N.; Jiang, Y. X.; Sun, S. G.; Ding, Y.; Wang, Z. L. *J. Am. Chem. Soc.* **2009**, *131*, 10860–10862.

(5) Massalski, T. B.; Okamoto, H. *Binary Alloys Phase Diagrams;* ASM International: Materials Park, OH; 1992.

(6) Wang, F. M.; Ingalls, R. *Phys. Rev. B* **1998**, *57*, 5647–5654.

(7) Laio, A.; Bernard, S.; Chiarotti, G. L.; Scandolo, S.; Tosatti, E. *Science* **2000**, *287*, 1027–1030.

(8) Vocadlo, L.; Alfe, D.; Gillan, M. J.; Wood, I. G.; Brodholt, J. P.; Price, G. D. *Nature* **2003**, *424*, 536–539.

(9) Cui, J.; Shield, T. W.; James, R. D. *Acta Mater.* **2004**, *52*, 35–47.

(10) Dudarev, S. L.; Bullough, R.; Derlet, P. M. *Phys. Rev. Lett.* **2008**, *100*, 135503.

(11) Park, H. S.; Kwon, O. H.; Baskin, J. S.; Barwick, B.; Zewail, A. H. *Nano Lett.* **2009**, *9*, 3954–3962.

(12) Ling, T.; Xie, L.; Zhu, J.; Yu, H. M.; Ye, H. Q.; Yu, R.; Cheng, Z. Y.; Liu, L.; Yang, G. W.; Cheng, Z. D.; Wang, Y. J.; Ma, X. L. *Nano Lett.* **2009**, *9*, 1572–1576.

(13) Ling, T.; Zhu, J.; Yu, H. M.; Xie, L. *J. Phys. Chem. C* **2009**, *113*, 9450–9453.

(14) Wen, Y. N.; Zhang, H. M. *Solid State Commun.* **2007**, *144*, 163–167.

(15) Wen, Y. N.; Zhang, J. M. *Comput. Mater. Sci.* **2008**, *42*, 281–285.

(16) Chen, Y. X.; Chen, S. P.; Chen, Q. S.; Zhou, Z. Y.; Sun, S. G. *Electrochim. Acta* **2008**, *53*, 6938–6943.

(17) Shibuta, Y.; Suzuki, T. *Chem. Phys. Lett.* **2007**, *445*, 265–270.

(18) Shibuta, Y.; Suzuki, T. *J. Chem. Phys.* **2008**, *129*, 144105.

(19) Finnis, M. W.; Sinclair, J. E. *Philos. Mag. A* **1984**, *50*, 45–55.

(20) Engin, C.; Sandoval., L.; Urbassek, H. M. *Modell. Simul. Mater. Sci. Eng.* **2008**, *16*, 035005.

(21) Leach, A. R. *Molecular Modelling: Principles and Applications*; Prentice-Hall: London, 2001.

(22) Evans, D. J.; Holian, B. L. *J. Chem. Phys.* **1985**, *83*, 4069–4074.

(23) Swope, W. C.; Anderson, H. C.; Berens, P. H.; Wilson, K. R. *J. Chem. Phys.* **1982**, *76*, 637–649.

(24) Qi, Y.; Cagin, T.; Johnson, W. L.; Goddard, W. A. *J. Chem. Phys.* **2001**, *115*, 385–394.

(25) Wen, Y. H.; Fang, H.; Zhu, Z. Z.; Sun, S. G. *Phys. Lett. A* **2009**, *373*, 272–276.

(26) Shim, J. H.; Lee, B. J.; Cho, Y. W. *Suf. Sci.* **2002**, *512*, 262–268.

(27) Xiao, S. F.; Hu, W. Y.; Yang, J. Y. *J. Phys. Chem. B* **2005**, *109*, 20339–20342.

(28) Wen, Y. H.; Fang, H.; Zhu, Z. Z.; Sun, S. G. *Chem. Phys. Lett.* **2009**, *471*, 295–299.

(29) Honeycutt, J. D.; Andersen, H. C. *J. Phys. Chem.* **1987**, *91*, 4950–4963.

(30) Schiotz, J.; Di Tolla, F. D.; Jacobsen, K. W. *Nature* **1998**, *391*, 561–563.

(31) Wen, Y. H.; Zhang, Y.; Zheng, J. C.; Zhu, Z. Z.; Sun, S. G. *J. Phys. Chem. C* **2009**, *113*, 20611–20617.

(32) Milstein, F.; Fang, H. E.; Marschall, J. *Philos. Mag. A* **1994**, *70*, 621–639.

(33) Hayat, S. S.; Choudhry, M. A.; Ahmad, S. A. *J. Mater. Sci.* **2008**, *43*, 4915–4920.

(34) Shibuta, Y.; Takamoto, S.; Suzuki, T. *ISIJ International* **2010**, *48*, 1582–1591.

(35) Li, S. Z.; Ding, X. D.; Li, J.; Ren, X. B.; Sun, J.; Ma, E. *Nano Lett.* **2010**, *10*, 1774–1779.

(36) Engin, C.; Urbassek, H. M. *Comput. Mater. Sci.* **2008**, *41*, 297–304.

(37) Kadau, K.; Gruner, M.; Entel, P.; Kreth, M. *Phase Transitions* **2003**, *76*, 355–365.

JP107709Q